ASEAN Engineering Journal

Full Paper

OPTIMIZATION OF CYLINDRICAL TUBE - PHASE CHANGE MATERIAL STORAGE FOR ENHANCED PERFORMANCE IN ASPHALT PAVEMENT THERMOELECTRIC HARVESTING

Putra Hariz Haikal Md Suraini[a], Khairun Nisa Khamil[a*], Azdiana Md Yusop[a], Mohd Afzanizam Mohd Rosli[b], Mohd Faizul Mohd Sabri[c], Ahmad Nizam Isa[d]

[a]Faculty of Electronics and Computer Technology and Engineering, Universiti Teknikal Malaysia Melaka, Hang Tuah Jaya, 76100 Durian Tunggal, Melaka, Malaysia.
[b]Faculty of Mechanical Technology and Engineering, Universiti Teknikal Malaysia Melaka, Hang Tuah Jaya, 76100 Durian Tunggal, Melaka, Malaysia.
[c]Faculty of Engineering, Universiti Malaya, 50603, Kuala Lumpur, Malaysia.
[d]Jabatan Kesihatan Negeri Melaka, Jalan Business City, Bandar MITC, 75450 Ayer Keroh, Melaka, Malaysia

Article history
Received
21 March 2025
Received in revised form
17 October2025
Accepted
23 October 2025
Published online
31 May 2026

*Corresponding author
nisa@utem.edu.myr

Graphical abstract

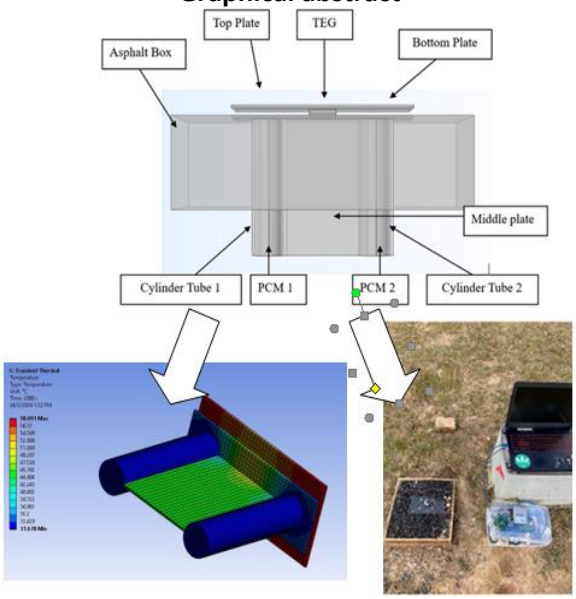

Abstract

Recent attention has focused on harnessing thermal energy from asphalt pavement due to its significant waste heat output. While studies have analyzed structural shape effects on heat conduction, the critical quantitative influence of the Phase Change Material's volume fraction on the overall thermal performance of the system structure remains unelaborated, hindering optimal thermal design. This study explores a thermoelectric energy harvesting system (TEH) designed to capture heat from asphalt surfaces. The project aimed to enhance TEH efficiency by incorporating phase change material (PCM) for subterranean cooling retention through simulation and experimentation. The design comprised an asphalt base holder, a top plate for heating, and a bottom plate for cooling. The top plate absorbs sunlight heat, while the bottom plate is submerged in the pavement and connected to a cooling element containing PCM. Finite Element Analysis (FEA) simulation and experimental validation were used for heat transfer analysis. Two PCM types, organic type (PCM A) and paraffin wax (PCM B), were employed, with PCM B demonstrating superior performance, yielding a higher temperature difference. The utilization of PCM B significantly advanced system performance, generating an average output voltage of 1.7 V and a temperature difference (ΔT) of 27.9 °C, an improvement of 12.71°C over previous studies which enabled the charging of a 5 F supercapacitor to 3.8 V in 2.50 hours., showcasing a notable advancement.

Keywords: word, thermoelectric system, energy harvesting, phase change material storage

1.0 INTRODUCTION

Thermoelectric devices are gaining significant attention for their potential in road infrastructure energy harvesting, converting waste heat dissipated from asphalt surfaces into useful electrical energy based on the Seebeck effect principle. This technology offers a sustainable pathway for applications such as independent power supply for remote sensors and IoT devices, which is particularly relevant in fluctuating climates like Malaysia [16]. However, the output power relies heavily on maintaining a large and stable temperature difference ΔT between the hot side (asphalt surface) and the cold side (subterranean environment). Integrating Phase Change Materials (PCM) is a promising approach to add dynamism to energy storage, improving heat regulation and thermoelectric efficiency by stabilizing the critical cold-side temperature [1, 2].

Prior research by Khamil et al. [3, 4] demonstrated the potential of a Thermoelectric Energy Harvesting System (TEHs) at asphalt pavement, stressing the importance of geometric design in heat extraction. These studies focused on using basic structures like aluminum plates and rods to conduct and dissipate subterranean heat [5]. Similarly, general research confirms that thermoelectric conversion efficiencies are heavily dependent on the efficiency of the TEM's cold side cooling system [6]. While PCM is attractive due to its high latent heat and cost-effectiveness [6], a comprehensive review by Luo et al. [7] highlighted a research gap: most current work focuses on PCM for heat absorption and cooling at high temperatures, necessitating more investigation into its role in low-temperature heat storage for cold-side applications. Specific material and design studies have proposed hybrid foam/PCM composites for thermal control [9] and two-stage storage tanks for fast solidification [8][20][21][22].

Despite advancements in pavement TEHs and PCM technology, a significant knowledge gap remains, particularly regarding the cold-side module design. Previous studies by Khamil et al. utilized only simple aluminum rods or varied geometric shapes for subterranean cooling, failing to leverage the dynamic thermal inertia of PCM [3][5]. Furthermore, a critical question left unanswered by existing literature [10][11] concerns the optimal amount of PCM to be filled within a containment structure, and how this quantity will influence the system's performance once submerged in the subterranean level. The latent heat effect for PCM-based storage at the underground level, particularly within a customized cylindrical structure, has yet to be explored to maximize ΔT effectively [23][24][25]. In a study by Li et al. show that PCM is used to store the latent heat to manipulate and stabilize the thermoelectric module's hot-side temperature to enhance the thermal conductivity and accelerate the heat dissipation [12].

Therefore, the primary objective of this paper is to enhance the thermoelectric output power of the asphalt pavement harvesting system. This will be achieved by upgrading the cold-side cooling module using a PCM-based storage system contained within a specific aluminum tube geometry instead of simple rods. The goal is to maximize the stable temperature difference ΔT across the TEG, leading to higher output power generation. The project's methodology entails a multi-stage approach designed to validate the enhanced cooling module. Initially, the proposed system, which integrates a Thermoelectric Generator (TEG) and a PCM-based storage module contained within an aluminum tube, will be modeled. The critical step involves optimizing the prototype design using ANSYS Simulation to precisely determine the most effective volume and placement of the PCM fill, focusing on how the cylindrical aluminum geometry influences heat conduction and thermal buffering. The simulation results will then be verified through controlled field testing for real-world applicability and performance measurement. This research offers several significant contributions: it is the first study to specifically explore and quantify the latent heat effect of PCM-based thermal buffering in the subterranean environment using a customized tubular aluminum geometry, providing a clear pathway to maximizing the stable ΔT. Furthermore, it delivers a validated, optimized design for a high-efficiency cold side module, offering a foundational system design for the independent power supply of low-power IoT devices embedded within asphalt pavement infrastructure.

2.0 METHODOLOGY

The methodology builds upon established thermal management techniques for pavement harvesting systems, specifically similar configuration employed in prior research [18][19]. This project introduces a critical upgrade to the conventional subterranean cooling module by replacing the inert aluminum cylindrical tubes with a novel Phase Change Material (PCM)-based storage system enclosed within an aluminum tube

2.1 Model of the Project

The proposed design in Figure 1 concept involves the direct exposure of the top aluminium plate to the asphalt surface, with its edge in direct contact with the asphalt. The thermoelectric cooling (TEC) [3, 4] was positioned between the top aluminium plate and the bottom aluminium plate. Prior research has extensively confirmed the use of the cooling element method, whereby an H-shaped configuration was formed through the fusion of an aluminium plate with two cylindrical tubes with a radius of 19.5 mm. Table 1 and 2 outlines the dimensions of the model with materials and the properties used in the simulation.

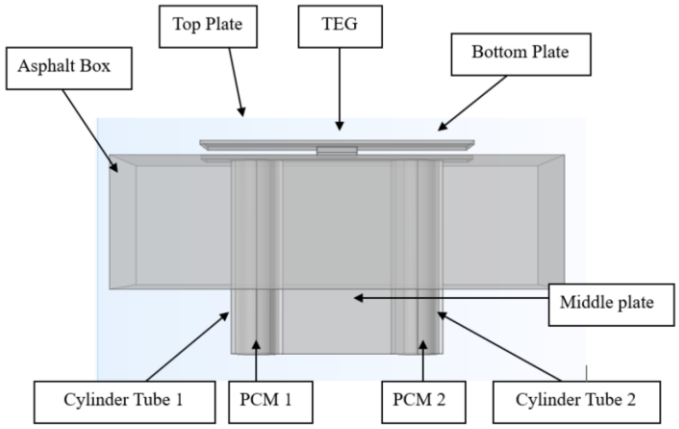

Figure 1 Simulation model TEHs at Asphalt Pavement.

Table 1 Dimensions of Simulation Model

Type	Dimension (mm)
Bottom Plate	60 x 200 x 3
Middle Plate	153 x 100 x 3
Cylindrical Tubes	Radius 19.5, Height 153
TEG Module	3 x 3 x 0.5
Top Plate	100 x 200 x 3
Asphalt	300 x 300 x 100

Table 2 Materials and Properties of the Simulation Model

Material	Density (kg/$m3$)	Heat Capacity (J/(kg.K))	Thermal Conductivity (W/(m.k))	Electrical Conductivity (S/m)	Melting Point (°C)	Latent Heat (kJ/kg)
Aluminium	2.7	900	222	3.77E+07	-	-
Alumina	2820	896	138	3.03E+07	-	-
Asphalt	2.24	900	0.8	-	-	-
PCM A	770	0.2	1500	-	25	230
PCM B	880	0.2	2000	-	30	170

2.2 Setup of the project for Field Testing

This project's experimental phase has been divided down into five parts. A model is made in the first section using PCM A and a clear surface top plate. The second section then includes a model with PCM A, and a surface top plate painted black. A model with a clear surface top plate and PCM B is the subject of the third section, and a model with a black-painted surface top plate and PCM B is the subject of the fourth. The experiment's fifth and final section involves using the model with a surface top plate painted black and PCM B to charge a supercapacitor. Each of these studies were completed over a period of 3 days, with a total of 2.5 hours dedicated to each day. The entirety of the acquired data was retained and subjected to analysis. As seen in Figure 2, the placement point of temperature sensors is presented in yellow star with detail stated in the figure

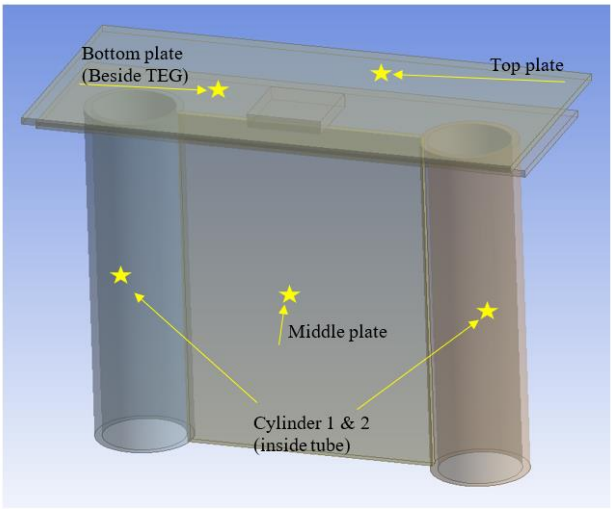

Figure 2 Placement of temperature sensors for both experiments and simulations

3.0 RESULTS AND DISCUSSION

3.1 Comparison of Simulations PCM A and PCM B Results

Figures 3 and 4 below show the results obtained from the result of the model tested for 2.5 hours of simulation using Thermal Transient in the ANSYS Engineering Simulation Software, with solar irradiance set based on an external radiation source.

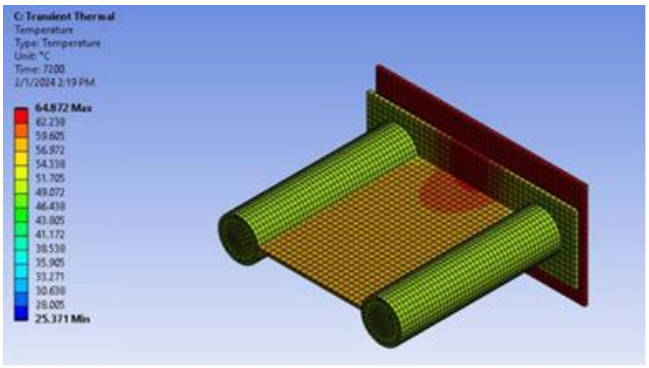

Figure 3 The Temperature Flow in Model with PCM A

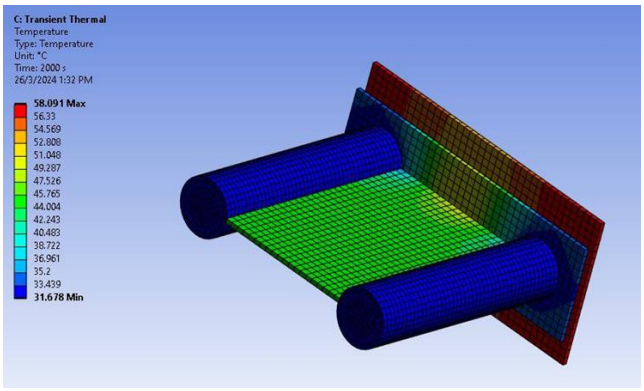

Figure 4 The Temperature Flow in Model with PCM B

Table 3 Summary Temperature Each Sides and Temperature Difference both Simulations

Type of PCMs	Duration (hour)	Top Plate Avg (°C)	Bottom Plate Avg (°C)	Middle Plate Avg (°C)	Cylinder 1&2Avg (°C)	ΔT (°C)
PCM A	0	25.4	25.4	25.4	25.4	0
	2	61.8	54.8	52	43.1	18.7
PCM B	0	25.4	25.4	25.4	25.4	0
	2	63.8	56.1	50.9	39.8	24.0

From the simulation of the model, the Table 3 summarizes the simulated temperature readings on two sides of a plate and the temperature difference between them. The experiment likely compared two different Phase Change Materials (PCMs), denoted as PCM A and PCM B. PCMs are materials that store and release thermal energy by changing their state, often from solid to liquid. The table shows that after 7200 seconds (2 hours) of simulation, both PCM A and PCM B resulted in a significant temperature difference between the top and bottom plates. PCM B appears to have resulted in a larger temperature

difference (24.0°C) compared to PCM A (18.7°C) after 2 hours, suggesting it may be more effective for thermal applications. Overall, the table helps assess the thermal performance of the two PCMs within the simulated model. PCMs with larger temperature differentials are generally considered more desirable for thermal. management applications. Hence, before verifying these results in field experiment, optimization for the size of top plate, both cylinders and PCMs in DOE carried out to see the most suitable and efficient geometry of the model.

3.2 Optimization in Design of Experiments (DOE)

A Design of Experiments (DOE) study can be employed within ANSYS to efficiently sample a design space. This approach allows for the construction of a statistical model capable of predicting desired responses (e.g., maximum stress, first natural frequency, maximum temperature) for a given design. DOE proves particularly valuable in scenarios where computational resources limit the number of feasible simulations. The core principle of DOE lies in strategically distributing these simulations (samples) across the design space. This strategic placement minimizes the uncertainty associated with the resulting statistical model, thereby enhancing its predictive accuracy. The Latin Hypercube Sampling (LHS) and Optimal Space Filling methods within the DOE framework will be utilized with user-defined parameters. A key benefit of these techniques is that the required number of simulations remains independent of the number of parameters being investigated.

3.2.1 Optimization for Model with PCM A

According to the Table 4, Design Point 0 (DP 0) had the highest temperature difference (ΔT), which was 17.2°C. In addition, DP 5 represents the minimum ΔT, which is 11.6°C. According to the theory of surface area to volume ratio, objects with larger surface areas can dissipate more heat. This is due to the fact that a greater surface area offers increased capacity and locations for heat transfer, whether it be heating loss or heat gain, depending on the surrounding conditions [2]. So that, DP 0 is the most suitable and efficient measurement of the top plate, both cylinders and both PCMs to conduct field experiment than other design points.

3.2.2 Optimization for Model with PCM B

Moving to optimization for model with PCM B, same as Table 5, the DP 0 is the most efficient in term of measurement of the model to generate the most ΔT between top plate and PCM. Hence, DP 0 dimensions will be chosen for field experiment.

3.3. Field Experiment Result

In the experiment as seen in Figure 5, temperature and voltage output are tracked for 2.5 hours, or 9000 seconds (12 pm to 2.30 pm GMT+8). The temperature data is collected using the PicoLog TC-08 data logger system, which yields the findings. For voltage output, the National Instrument DAQExpress companion software is used. To ensure the consistency of the results, each experiment was carried out for a duration of three days. This was done by conducting the experiment multiple times, which aids in discerning whether the observed data was an anomaly or indicative of the norm. In this study, Mean Absolute Percentage Error (MAPE) is used to analyzed the average of absolute errors divided for each day experiment values

Table 4 Optimization in DOE for Model with PCM A

Name	Top Plate width x length (mm)	Cylinder 1&2 (mm)	PCM 1&2 (mm)	Top Plate Max Temp (°C)	PCM Max Temp (°C)	ΔT (°C)
DP 0	200 x 100	19.5	16.5	61.7	44.5	17.2
DP 1	210 x 110	20.0	17.0	60.4.	44.5	15.9
DP 2	220 x 120	21.0	18.0	57.9	44.5	13.4
DP 3	230 x 130	22.0	19.0	57.0	44.5	12.5
DP 4	240 x 140	23.0	20.0	56.7	44.5	12.2
DP 5	250 x 150	24.0	210	56.1	44.5	11.6

Table 5 Optimization in DOE for Model with PCM B

Name	Top Plate width x length (mm)	Cylinder 1&2 (mm)	PCM 1&2 (mm)	Top Plate Max Temp (°C)	PCM Max Temp (°C)	ΔT (°C)
DP 0	200 x 100	19.5	16.5	61.7	38.1	23.6
DP 1	210 x 110	20	17	60.4	38.1	22.3
DP 2	220 x 120	21	18	57.9	38.1	19.8
DP 3	230 x 130	22	19	57.0	38.1	18.9
DP 4	240 x 140	23	20	56.7	38.1	18.6
DP 5	250 x 150	24	21	56.1	38.1	18

Figure 5 Data collection setup in field testing

Figure 6 Overview of H-Shaped Heat Sink with Aluminium Tube as PCM Storage with Asphalt mock-up

The internal overview of the system is presented in the Figure 6 to validate the simulation done.

The experiments have 5 parts of results which consists of:

i. Model with clear surface top plate and PCM A.
ii. Model with black painted surface top plate and PCM A.
iii. Model with clear surface top plate and PCM B.
iv. Model with black painted surface top plate and PCM B.
v. Charging Supercapacitor using the model with black painted surface top plate and PCM B.

3.3.1. Part 1: Experiment Result for Model with clear surface top plate using PCM A

The Table 6 shows the average temperature readings for a thermoelectric generator (TEG) experiment across three days The TEG uses temperature differences to generate electricity. The readings were taken from various locations on the TEG unit, including top and bottom plates, a middle plate, cylinder walls, and the asphalt surrounding the TEG. Additionally, the table includes a measurement called ΔT (°C), which likely refers to the temperature difference between the top plate and Day 1 has the highest average ΔT (°C), indicating the largest temperature difference between the top plate and the cylinders. This suggests that Day 1 may have been the most efficient day for TEG electricity generation. The average daily temperature on Days 2 and 3 is lower than Day 1, possibly due to partly cloudy weather as mentioned in the passage below the table. The overall MAPE% is 25.53, which may indicate a moderate level of error in the temperature readings. Overall, the table helps assess the thermal performance of the TEG unit across the three-day experiments and further elaboration on the average output voltages are presented in the Table 8.

Table 6 Average Temperature for Whole Model for Three Days

	Top Plate (°C)	Bottom Plate (°C)	Middle Plate (°C)	Cylinder 1&2 (°C)	Asphalt (°C)	ΔT (°C)
Day 1	54.3	31.4	30.7	30.3	53.7	20
Day 2	47.6	30.5	30.1	31.3	48.2	16.3
Day 3	51.4	34.7	33.7	33.9	47.4	17.5
MAPE %	8.65	8.72	7.61	7.41	8.4	25.53

3.3.2 Part 2: Experiment Result for Model with Black Painted Surface Top Plate using PCM A

Table 7 shows that the average daily temperature readings for Days 2 and 3 seem lower than Day 1. The experiment appears to have achieved its highest average temperature difference (ΔT °C) on Day 3, possibly indicating the most efficient day for thermal energy generation. In this table, the MAPE % for the Top Plate, Bottom Plate, and Middle Plate are all below 6%, indicating a good level of accuracy for those measurements. However, the Cylinder 1&2 and Asphalt average temperature have higher MAPE %, around 9% and 11% respectively but still within that acceptable range. Hence, the output voltage for these measurements using higher emissivity top plate is investigated and analyzed in the next table to see how much it has influence in the results.

Table 7 Average Temperature for Whole Model for Three Days

	Top Plate (°C)	Bottom Plate (°C)	Middle Plate (°C)	Cylinder 1&2 (°C)	Asphalt (°C)	ΔT (°C)
Day 1	49.8	33.2	32.7	30.1	48.2	19.7
Day 2	55.7	35.2	33.9	34.4	53.1	21.3
Day 3	56.3	36.1	34.7	32.9	55.9	23.4
MAPE %	8.16	5.54	3.93	9.05	9.74	11.26

Table 8 Average output voltage for TEG and boosted voltage for both clear and painted surface for PCM A

	VTeg (V) Clear Surface	Vboost (V) Clear Surface	VTeg (V) Painted Surface	Vboost (V) Painted Surface
Day 1	0.9	3.9	1.1	4.8
Day 2	1.3	5.0	1.2	5.0
Day 3	0.8	3.7	1.3	5.0

The Table 8 depicted that the boosted voltage appears to be consistently higher than the TEG's output voltage (VTeg) for both clear and painted surfaces, indicating that the booster circuit is functioning as expected. The highest output voltage and boosted voltage occurred in Day 3 of experiment for Painted surface which proven the Stefan-Boltzmann Law with 1.3V of VTeg and ΔT of 23.4°C. This also related to the Seebeck effects: with larger the temperature difference between the hot and cold sides of a TEG, the greater the induced voltage difference. Hence, in the next part, another key factor that will be look into is different materials of PCM.

A top plate with high emissivity (close to 1) acts like a good radiator. It efficiently converts its internal thermal energy into infrared radiation and emits it at a rate predicted by the Stefan-Boltzmann Law for its temperature. As for clear surface top plate, with low emissivity (much less than 1) acts like a poor radiator. It absorbs most of its internal heat and struggles to emit it as radiation. As a result, the top plate surface might feel hot to the touch even though it's not radiating much heat according to the Stefan-Boltzmann Law where the law applies to ideal black bodies, which perfectly absorb and emit all radiation falling on them. However, real objects like a top plate surface rarely behave like perfect black bodies. Emissivity is a property of a material that describes how efficiently it emits radiation compared to a black body at the same temperature [13]. Therefore, in next part are the studies of different PCM materials using both clear surface and black painted surfaces.

3.3.3 Part 3: Experiment Result for Model with clear surface top plate using PCM B

As seen in Table 9 show the readings of MAPE has the highest percentage at 32°C. This happened due to high difference of ΔT in Day 2 that contribute to the rise in MAPE. On Day 2, the weather was cloudy and slight colder than usual due to rainy days on the night before. The output and boosted voltage may demonstrate the result to support the temperature variation for this incident in Table 12.

Table 9 Temperature variation for clear surface top plate and PCM B

	Top Plate (°C)	Bottom Plate (°C)	Middle Plate (°C)	Cylinder 1&2 (°C)	Asphalt (°C)	ΔT (°C)
Day 1	50.3	35.7	35.1	33.1	50.8	17.2
Day 2	43.9	32.9	33	32.8	40.2	11.1
Day 3	47.5	36	34.7	29.9	45.6	17.6
MAPE	8.94	6.03	4.1	6.82	15.23	32.1

3.3.4 Part 4: Experiment Result for Model with black painted surface top plate using PCM B

In Table 10, using PCM B with Melting point of 30°C display the TEH results obtained has the highest ΔT from all the other conducted experiments. These have demonstrated better performance and as well as improved the system performances

Table 10 Average Temperature variation for painted top plate surface using PCM B

	Top Plate (°C)	Bottom Plate (°C)	Middle Plate (°C)	Cylinder 1&2 (°C)	Asphalt (°C)	ΔT (°C)
Day 1	61.7	47.3	43.8	33.8	60.2	27.9
Day 2	58.3	38.9	35.3	32.6	58.7	25.7
Day 3	57.9	43.1	37.6	33.3	58.9	24.6
MAPE	4.25	12.77	14.14	2.4	1.68	8.53

Table 11 Average output voltage for TEG and boosted voltage for both clear and painted surface for PCM B

	VTeg (V) Clear Surface	Vboost (V) Clear Surface	VTeg (V) Painted Surface	Vboost (V) Painted Surface
Day 1	1.3	5	1.7	5
Day 2	0.5	3.9	1.6	5
Day 3	1.4	5	1.7	5

According to the obtained result presented in Table 11, TEHs with PCM B melting point have higher output voltage than TEHs with PCM A. The PCM thermal storage with PCM B retained at below 40 °C during the 2.5 hours of experiment aided by the black painted surface top plate. The black painted surface has absorbed heat than clear surface. The difference between PCM A and PCM B are the types of PCM where the PCM A is an organic type and PCM B is inorganic. Hence, the organic PCMs may have a lower thermal conductivity, indicating that these materials may transfer heat less efficiently [13]. Therefore, the clear surface top plate is not suitable because has low surface emissivity and PCM A is unsuitable as PCM thermal storage temperatures are extremely high. Lastly, TEHs with black painted top surface with PCM B were chosen to test the new system's charging capabilities.

3.3.5 Part 5: Experiment Result For Charging Supercapacitor Using The Model With Black Painted Surface Top Plate And PCM B

The final experimental phase evaluated the charging performance of the TEHs, which was configured with the black-painted surface top plate and PCM B, by channelling its output into two series-connected 5F, 2.5V supercapacitors. The integration of PCM B with a black-painted top plate sustained a top-to-bottom plate temperature difference of 25.7°C as shown in Table 12, enabling the TEH system to generate a 2V output that successfully charged the supercapacitor to 3.8 V via the boost converter, BQ25505 detailed in Table 13.

This circuit was essential for efficiently extracting the generated µW to mW level power without causing source collapse [17]. Critically, the BQ25505 also provided indispensable safety and management features, preventing the supercapacitors from being either overcharged by the boosted

voltage or depleted beyond their safe operational limits by the system load. The open circuit voltage from the thermoelectric is connected directly to the power management circuit (PMC) and then the supercapacitor is connected to the battery pin for the safety features as mentioned. The physical and electrical connections for the charging test are shown in Figure 7.

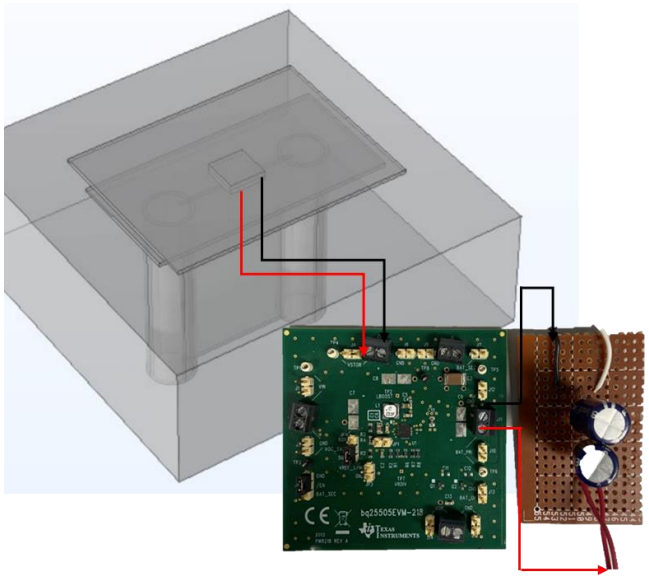

Figure 7. Block Diagram of the Power Management Circuit (PMC) and Supercapacitor connection.

Table 12 Average Temperature for charging capabilities using painted surface top plate with PCM B

Top Plate Avg (°C)	Bottom Plate (°C)	Middle Plate (°C)	Cylinder 1&2 (°C)	Asphalt (°C)	ΔT (°C)
59.7	36.7	34.9	34	57.9	25.7

Table 13 Data Collected for experiment to charge supercapacitor using the TEHs. with and black painted top plate and PCM B

Vteg (V)	Vboost (V)	VCap (V)
2	4.3	3.8

One of the most important things learned from this study is that black painted surface top plate with PCM B was used to charge two 5F supercapacitors in series. Study shows with the average output voltage (VTeg) of 2V, the system able to boost till 4.3V within 2.5 hours and charge the supercapacitor till 3.8V which enough to supply a low power device that only requires the same amount.

3.4 Findings of the experiment

Table 14 presents the comparison between the average result from the 3-day experiment and the simulation to validate the findings. It is evident from both tables that the experimental temperature differences are marginally greater than those predicted by the simulations.

Table 14 Comparison between Simulation and Experimental Results for TEHs with both PCMs

Type of PCMs	Simulation ΔT (°C)	Experimental ΔT (°C)	Error (%)
PCM A	18.7	21.4	14.4
PCM B	24.0	26.0	8.3

The prime aim of this project is to design a better TEHs at asphalt pavement with greater performance of the TEG. Referring to Equation 1, the bigger the temperature difference between the cold side of the TEG, which in this experiment, is the bottom plate, and the hot side of the TEG, which is the top plate in this experiment, the greater the output voltage from the TEG. In comparison for PCM A and B presented in Table 15, PCM B shows a superior and far more accurate than PCM A.

Table 15 Comparison Both Analysis with PCMs and Previous Article [2]

Item	Simulation ΔT (°C)	Experiment ΔT (°C)
PCM A	18.7	21.4
PCM B	24.0	26.0
Previous Article [3]	12.8	15.19

Hence, this proved that PCM does influence the TEHs to retain the subterranean cooling and produce greater temperature difference between the hot side and the cold side of the TEG. This is because, in theory, PCM can retain the cold side of the TEG by acting as cold storage. It can be seen that the method drastically improves the performance of the compared to previous system.

3.5 Discussion

Two types of phase change material (PCM) are examined in this study: PCM A and PCM B (paraffin wax). PCM B, with a black painted surface top plate, achieves an average output voltage of 1.2V and a temperature difference (ΔT) of 21.4°C, while PCM A, with a clear surface top plate, only manages 1.0V and a ΔT of 19.2°C. PCM B, also with a black painted surface top plate, outperforms PCM A with an average output voltage of 1.6V and a ΔT of 26.0°C compared to 1.2V and 15.3°C, respectively, for the clear surface top plate with PCM B. The inferior thermal conductivity of PCM A suggests less efficient heat transfer for PCM types. PCM B, an inorganic paraffin wax, offers superior thermal conductivity and stability compared to PCM A, an organic material. Its inorganic composition ensures better heat transfer and stability in fluctuating temperatures, leading to increased voltage outputs [13]. Conversely, PCM A may exhibit lower thermal conductivity and stability due to its organic composition, highlighting the superiority of inorganic PCM B for applications requiring consistent thermal performance. Emissivity, quantifying a material's ability to emit thermal radiation, is crucial in understanding heat interactions [14]. A black surface, with an emissivity of 1, emits thermal radiation most effectively, while a clear surface emits less. This emphasizes the effectiveness of black surfaces in thermal regulation applications. PCM B has effectively charges two 5F supercapacitors in series, requiring approximately 3.3V and achieving up to 4.1V in over 2.5 hours, a significant finding of this study. This hybridization in PCM also suggested in [15] which exhibits superior performance in terms of voltage output and temperature difference.

3.6 Sustainability

By successfully charging of two 5F supercapacitors in series using PCM B highlights the potential of this system for practical energy harvesting applications, contributing to SDG 7: Affordable and Clean Energy by exploring sustainable and renewable energy sources.

The key sustainability aspects highlighted in this study include:

Material Selection: The research emphasizes the importance of choosing PCMs with high thermal conductivity and stability, such as inorganic materials like paraffin wax, for improved performance and durability.

Surface Treatment: The use of black surfaces enhances thermal radiation absorption and emission, maximizing energy conversion and improving overall system efficiency.

Energy Storage: The successful charging of supercapacitors demonstrates the feasibility of integrating PCM-based energy harvesting systems with energy storage devices, enabling continuous power supply and improving system reliability.

4.0 CONCLUSION

This study addressed efficiency limitations in thermoelectric generators (TEGs) by employing finite element analysis (FEA) to simulate the effect of an aluminium tube with phase change material (PCM) on thermoelectric output. The design of experiment (DOE) in ANSYS Simulation enhanced the prototype's structure, verified through field testing. The use of PCM reduced temperature fluctuations, leading to improved voltage output. The study achieved its goals and proposed a method to enhance thermoelectric output for road harvesting, advancing sustainable energy technology. For further considerations in the next study will be the life-cycle assessment of the PCMs and the entire energy harvesting system where it is necessary to evaluate the environmental impact and overall sustainability. The scalability and integration of PCM-based energy harvesting systems into real-world applications should be further investigated as well in the next study such as building facades or road infrastructure, is crucial for practical implementation and wider adoption of SDG 7: Affordable and Clean Energy.

Acknowledgement

This research is sponsored by Kementerian Pengajian Tinggi Malaysia (KPT) and Universiti Teknikal Malaysia Melaka under grant: FRGS/1/2023/TK08/UTEM/02/4

Conflicts of Interest

The author(s) declare(s) that there is no conflict of interest regarding the publication of this paper

References

[1] Sharma, S., Dwivedi, V. K., & Pandit, S. N. 2014. A review of thermoelectric devices for cooling applications. *International Journal of Green Energy*, *11*(9): 899–909.

[2] Sasidharan, M., Mohd Sabri, M. F., Wan Muhammad Hatta, S. F., & Ibrahim, S. 2024. A review on the progress and development of thermoelectric air conditioning system. *International Journal of Green Energy*, *21*(2): 283–299.

[3] Khamil, K. N., Isa, A. N., Yusop, A. M., & Mohd Sabri, M. F. 2021. Influence of conduction shape factor in subterranean cooling for a thermoelectric energy harvesting system at asphalt pavement: An experimental investigation. *Energy Sources, Part A: Recovery, Utilization, and Environmental Effects*: 1–18.

[4] Khamil, K. N., Mohd Sabri, M. F., & Yusop, A. M. 2024. Thermoelectric energy harvesting system (TEHs) at asphalt pavement with a subterranean cooling method. *Energy Sources, Part A: Recovery, Utilization, and Environmental Effects*, *46*(1): 10662–10678.

[5] Khamil, K. N., Mohd Sabri, M. F., Md Yusop, A., Mohd Sa'at, F. A. Z., & Isa, A. N. 2021. High cooling performances of H-shape heat sink for thermoelectric energy harvesting system (TEHs) at asphalt pavement. *International Journal of Energy Research*, *45*(2): 3242–3256.

[6] Sajid, M., Hassan, I., & Rahman, A. 2017. An overview of cooling of thermoelectric devices. *Renewable and Sustainable Energy Reviews*, *78*: 15–22.

[7] Luo, J., Zou, D., Wang, Y., Wang, S., & Huang, L. 2022. Battery thermal management systems (BTMs) based on phase change material (PCM): A comprehensive review. *Chemical Engineering Journal*, *430*: 1–18.

[8] De Falco, M., Salvatori, M., & Zaccagnini, A. 2021. Experimental investigation of a multi-kWh cold storage device based on phase change materials. *Journal of Energy Storage*, *41*: 1–12.

[9] Li, W. Q., Zhang, T. Y., Li, B. B., Cui, F. Q., & Liu, L. L. 2021. Experimental investigation on combined thermal energy storage and thermoelectric system by using foam/PCM composite. *Energy Conversion and Management*, *243*: 1–9.

[10] Xiaofeng, X., & Xuelai, Z. 2021. Simulation and experimental investigation of a multi-temperature insulation box with phase change materials for cold storage. *Journal of Food Engineering*, *292*: 1–9.

[11] Cheng, T., Wang, N., Wang, H., Sun, R., & Wong, C. P. 2020. A newly designed paraffin@VO2 phase change material with the combination of high latent heat and large thermal conductivity. *Journal of Colloid and Interface Science*, *559*: 226–235.

[12] Zhu, M., Wang, Z., Zhang, H., Sun, X., Dou, B., Wu, W., … Jiang, L. 2022. Experimental investigation of the comprehensive heat transfer performance of PCMs filled with CMF in a heat storage device. *International Journal of Heat and Mass Transfer*, *188*: 1–14.

[13] Arabkoohsar, A. 2023. Classification of energy storage systems. In *Future Grid-Scale Energy Storage Solutions*: 1–30. Elsevier

[14] Kusuma, K. N. 2023. Emissivity. In *Encyclopedia of Lunar Science* : 258–262. Springer International Publishing.

[15] Guo, Y., Zhang, X., Wang, J., Yan, Y., & Ren, Y. 2023. Investigation of continuous pulse current source on the performance of phase change material-thermoelectric cooler system. *e-Prime - Advances in Electrical Engineering, Electronics and Energy*, *4*: 1–10.

[16] Yingsamphancharoen, T., Promdaung, W., & Bangyeekhan, S. (2025). An Electric Conversion Set Of Geothermal Energy Using A Thermoelectric Device: Case At A Hot Spring. *ASEAN Engineering Journal*, 15(1): 113-121.

[17] Texas Instruments. BQ25505 ultra low-power boost charger with battery management and autonomous power multiplexer for primary battery in energy harvester applications. https://www.ti.com/lit/gpn/bq25505. 2013. Accessed on December 23, 2024.

[18] Bakar, A. S. A., Khamil, K. N., Yusop, A. M., Rosli, M. A. M., & Sabri, M. F. M. (2025). An Analysis of Phase Change Material for Heat Retainment of Thermoelectric Energy Harvesting System at Asphalt Pavement. *Energy Storage*, 7(3): e70161.

[19] Zainurin, F. N. H. B., Khamil, K. N., Md Yusop, A., Rosli, M. A. B. M., Mohd Chaculi, S. A., & Mohd Sabri, M. F. (2024). An analysis of phase change material for subterranean cooling of the thermoelectric energy harvesting system at asphalt pavement. *International Journal of Ambient Energy*, 45(1).

[20] W.-X. Chu, I.-J. Chen, C.-T. Chan, J.-S. Wu, and C.-C. Wang. Experimental study on the energy harvesting of a cooktop via thermoelectric module assisted with phase change material, *Energy Storage*, vol. 1, no. 2: e55

[21] S. S. Kumar and G. A. P. Rao, "Recent progress on battery thermal management with composite phase change materials," *Energy*

Storage, vol. 6, no. 4: e647.

[22] J. Mao, A. Liu, Y. Wang, Y. Li, H. Xie, and Z. Wu. Enhancement of power generation of thermoelectric generator using phase change material, *IOP Conference Series: Materials Science and Engineering*, vol. 892: 012055

[23] F. J. Montero, R. Lamba, A. Ortega, W. Jahn, and A. M. Guzmán. A novel 24-h day-night operational solar thermoelectric generator using phase change materials, *Journal of Cleaner Production*, vol. 296: 126553

[24] Zalba, B., J. M. Marín, L. F. Cabeza, and H. Mehling. 2003. Review on Thermal Energy Storage with Phase Change: Materials, Heat Transfer Analysis and Applications. *Applied Thermal Engineering* 23 (3): 251–283.

[25] Yu, C., and Y. S. Song. 2023. Enhancing Energy Harvesting Efficiency of Form Stable Phase Change Materials by Decreasing Surface Roughness. *Journal of Energy Storage* 58: 106360.